Journal of Magnetism and Magnetic Materials 377 (2015) 490–495

Contents lists available at ScienceDirect

Journal of Magnetism and Magnetic Materials

journal homepage: www.elsevier.com/locate/jmmm

Microstructural and magnetotransport studies of novel manganite–sebacic acid nanocomposites prepared at low temperature

Mariano Romero [a,b], Ricardo Faccio [a,b], Helena Pardo [a,b], Milton A. Tumelero [c], André A. Pasa [c], Álvaro W. Mombrú [a,b,*]

[a] Centro NanoMat/Cryssmat Lab/Cátedra de Física – DETEMA – Facultad de Química – Universidad de la República, Uruguay
[b] Centro Interdisciplinario de Nanotecnología, Química y Física de Materiales – Universidad de la República, Uruguay
[c] Laboratorio de filmes finos e superficies – Departamento de Física – Universidad Federal de Santa Catarina, Florianópolis, Brazil

ARTICLE INFO

Article history:
Received 16 September 2014
Received in revised form
21 October 2014
Available online 6 November 2014

Keywords:
Manganite
Nano-composites
Magnetotransport

ABSTRACT

Novel $La_{2/3}Sr_{1/3}MnO_3$:sebacic acid nanocomposites (LSMO–SA-*X*) were prepared for different fraction additions (*X*) of sebacic acid (SA). The preparation of these nanocomposites was performed at low temperatures ($T \sim 130$ °C) avoiding partial decomposition of the organic matrix. The microstructure of these LSMO–SA-*X* nanocomposites was studied by small angle X-ray scattering (SAXS) technique and both nanoparticles size and inter-particle distances were estimated.

The magnetic, electrical and magnetotransport properties were also investigated. An enhancement in the low-field magnetoresistance (LFMR) for lower fractions of SA was obtained with respect to pure LSMO and higher fraction additions showed a decrease in the LFMR due to the higher separation distance between LSMO nanoparticles. The tunnel barrier thickness observed in these nanocomposites was correlated with the interparticle distance obtained by SAXS. The enhancement of magnetoresistance was attributed to the increase in the extrinsic disorder promoted by the SA addition and no enhancement due to intrinsic magnetoresistance of LSMO was evidenced.

1. Introduction

Research on the synthesis of polycrystalline manganites in which intergrain magnetoresistance significatively modified their physical properties has been an interesting matter of research [1–4]. The main characteristic of polycrystalline manganites is a high magnetoresistance values at low applied fields in a wide range of temperature below the insulator–metal transition. This grain boundary effect is absent in the crystal and it is associated to natural and artificial effects [5,6]. The spin polarized tunneling [1] and the spin-dependent scattering [5] between adjacent grains is assumed to be the responsible of this colossal magnetoresistance. This extrinsic effect that enhances the magnetoresistance at low applied fields in a wide range of temperatures could be useful for technological applications [7]. The tunneling process takes place through the interface of grains separated by an energy barrier related to magnetic disorder. On behalf of this, the addition of an insulating material between the manganite grains would adjust the barrier layer influencing the tunneling process. The insulator would act as fixing centers for demagnetization and the application of a low applied field could align ferromagnetic adjacent grains enhancing the magnetoresistance. For this reason, the spin disorder at the interface of the system is crucial to promote an increase in the magnetoresistance values at low applied fields. In spite of this, the magnetoresistance decreases rapidly with increasing temperature [8]. Several reports have been published looking for an enhancement of LFMR by the preparation of nanocomposites formed with a colossal magnetoresistance (CMR) oxide and secondary phases as insulating oxides, different CMR oxides [9–15] and polymers [8,16,17]. Nano-composites composed by manganites and polymer matrices have shown enhancing magnetoresitance at low temperatures with respect to manganites without the addition of secondary phases. A previous report for the $La_{2/3}Sr_{1/3}MnO_3$:PEG:PMMA system indicates that the polymer fraction has an optimal value in the magnetotransport effect associated to a relatively high magnetoresistance values. Additionally, higher fractions of polymer lead to a huge increase in the resistivity with grains well separated from each other [18]. Other studies of LSMO–PPP nano-composites [8] have demonstrated that polyparaphenylene (PPP) do not modify the transport mechanism but the grain boundary effect. Moreover, LCMO–PPS nano-composites [7] also showed that the increase of paraphenylsulfur (PPS) content leads to a shift in the insulator–metal

* Corresponding author at: Centro NanoMat/Cryssmat Lab/Cátedra de Física – DETEMA – Facultad de Química – Universidad de la República, Uruguay. .
E-mail address: amombru@fq.edu.uy (Á.W. Mombrú).

http://dx.doi.org/10.1016/j.jmmm.2014.11.001
0304-8853/

transition to lower temperatures without changing the Curie temperature.

The measurement of LFMR at 3 kOe showed an enhancement at low temperatures ($T=80$ K) of 18% for a 20% weight fraction of polymer respect to 16% for pure ceramic. Most reports are based on the preparation of LSMO–polymer nanocomposites including mixing and grinding of the polymer with LSMO nanoparticles followed by a thermal annealing at ~400 °C. In order to prepare highly homogeneous and less decomposed systems we are reporting the preparation of novel manganite–sebacic acid nanocomposites with thermal treatment at lower temperatures ($T\sim 130$ °C) than those that are commonly used for the preparation of these systems. Additionally, there are no reports regarding a strict characterization of the microstructure in these nano-composites. On behalf of this, we have performed small angle X-ray scattering (SAXS) measurements in order to find out the inter-particle distances in these nano-composites. These experiments would allow us to give relevant information about the tunnel barrier thickness. Magnetic, electrical and magnetotransport measurements are analyzed as a function of temperature and applied field. Magnetotransport properties are discussed in correlation with the microstructural characterization obtained using SAXS technique. Undoubtedly, the correlation of microstructure analysis with magnetotransport measurements is very useful to understand the transport mechanisms on these types of systems.

2. Materials and method

Analytical-grade lanthanum nitrate ($La(NO_3)_3\cdot 6H_2O$), strontium nitrate ($Sr(NO_3)_2$) and manganese nitrate ($Mn(NO_3)_2\cdot 4H_2O$) were dissolved in the desired ratio in a 100 mL flask with distilled water. Citric acid ($C_6H_8O_7\cdot H_2O$) and ethyleneglycol ($C_2H_6O_2$) were added to the solution and heated for 6 h at 100 °C until a gel was formed. This gel was calcinated with a 20 °C/min ramp rate at 1000 °C for 5 h in order to obtain $La_{2/3}Sr_{1/3}MnO_3$ nanoparticles, named as LSMO.

Nano-composites were prepared by mixing and grinding LSMO with a 0, 5, 10, 15 and 20% w/w of sebacic acid (SA). Samples were pressed into pellets at 50 kPa and then heated at 130 °C during 3 h. Samples were named LSMO–SA-*X*, being *X* the weight fraction of sebacic acid.

Structural analysis was performed by X-ray powder diffraction (XRPD) using a Rigaku Ultima IV diffraction system, with CuKα radiation in the range $2\theta=10°$–$100°$ with a 15 s step of 0.02° and Rietveld refinement was performed using GSAS-EXPGUI software package. Scherrer equation based in the Lorentzian component of Rietveld refinement $D=18{,}000K\lambda/\pi L_X$ was applied to obtain nanocrystallite mean size (D). GISAXS experiments were performed directly onto the LSMO–SA-*X* compressed pellets surface and were carried out using CuKα radiation ($\lambda=1.5418$ Å) in the scattering vector range $q=0.0074$–0.145 Å^{-1}. SAXS data analysis was performed using Debye [19–23] and a new Guinier–Porod models described elsewhere [24,25]. The Guinier part of the $I(q)$ versus q curve implemented at low-q region is given by Eq. (1) [25]:

$$I(q) = Ge^{-q^2R_g^2/3} \tag{1}$$

where G is a Guinier scale factor and R_g is the gyration radius for a sphere and the mean diameter of a spherical particle (L_P) is given by

$$D = L_P = \frac{2R_g}{\sqrt{3/5}} \tag{2}$$

The rough estimation of the correlation distance (L_S) at high-q region is given by Eq. (3) [23]:

$$\frac{2\pi}{q_{\max}} \le L_S \le \frac{2\pi}{q_{\min}} \tag{3}$$

The Porod part is given by

$$I(q) = Aq^{-P} \tag{4}$$

where A is the Porod scale factor and P is the Porod exponent [23].

Magnetization measurements were performed in a VSM-Microsense EV9 vibrating sample magnetometer. DC resistivity (R) measurements were taken in the 15–305 K temperature range by the four-probe technique and magnetoresistance (MR) was calculated as follows: $MR(\%)=100(R_H-R_0)/R_0$, with R_H and R_0 as the resistivity under transversal applied magnetic field ($0<H<4.5$ kOe) and without applied field, respectively.

3. Results and discussion

X-ray diffraction patterns of LSMO–SA-*X* samples showed the presence of the $La_{2/3}Sr_{1/3}MnO_3$ perovskite showing an orthorhombic structure with *Pbnm* spacegroup. No significant variations in the unit cell parameters were noticed for different SA additions suggesting that there are no relevant variations in manganese valence with the preparation treatment. Crystallite size (D) applying the Scherrer equation was $D\sim 27$ nm for LSMO nanoparticles and no variations were observed for all SA additions. All diffraction patterns (Fig. 1) showed the absence of SA crystalline peaks suggesting the formation of amorphous SA after thermal treating at 130 °C. This observation is in agreement with the SA melting filling the LSMO inter-particle spaces leading to a homogeneous nano-composite with no SA crystalline segregation. Nevertheless, very low intensity peaks in the $2\theta=20°$–$25°$ region were detected and assigned to partial decarboxylation of sebacic acid into caproic acid [26].

FT-IR spectra (Fig. 2) showed a broad peak at ~615 cm^{-1} ascribed to MnO_6 octahedra stretching modes of LSMO nanoparticles. Other peaks at ~1415 and 1543 cm^{-1} were attributed to asymmetric and symmetric stretching modes of carboxylate groups, respectively, and peaks at ~2900 and 3500 cm^{-1} were attributed to the ethylene and methylene stretching modes,

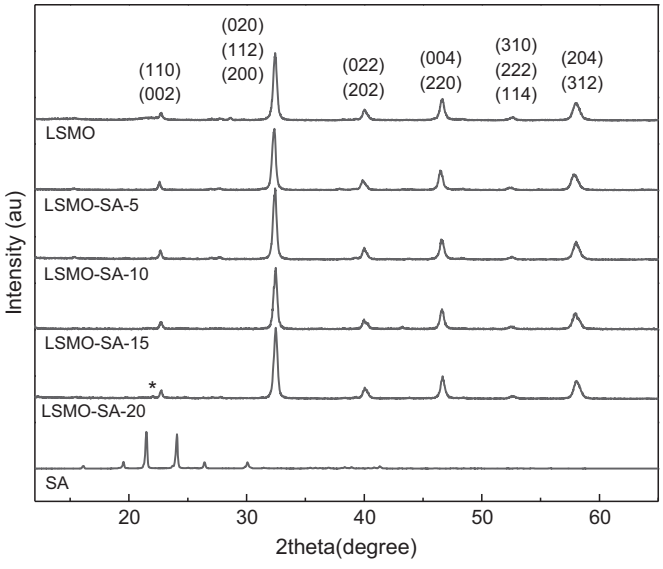

Fig. 1. XRPD patterns of LSMO–SA-*X*. The asterisk in LSMO–SA-20 pattern shows the diffraction peak corresponding to caproic acid.